

## Article

# Feasibility of the Production of *Argemone pleiacantha* Ultrasound-Assisted Biodiesel for Temperate and Tropical Marginal Areas

Javier Sáez-Bastante <sup>1</sup>, Miguel Carmona-Cabello <sup>1</sup>, Elena Villarreal-Ornelas <sup>2</sup>, Ricardo Trejo-Calzada <sup>2</sup> , Sara Pinzi <sup>1</sup>  and M. Pilar Dorado <sup>1,\*</sup> 

<sup>1</sup> Department of Physical Chemistry and Applied Thermodynamics, Escuela Politécnica Superior, Edificio Leonardo da Vinci, Campus de Rabanales, Universidad de Córdoba, Campus de Excelencia Internacional Agroalimentario, CeIA3, 14071 Córdoba, Spain

<sup>2</sup> Regional Unit of Arid Areas, Chapingo Autonomous University, Pueblo Bermejillo 35230, Dgo., Mexico

\* Correspondence: pilar.dorado@uco.es; Tel.: +34-957218332

**Abstract:** The present work studies biofuel production using an American native species that belongs to the *Argemone* genus. It is considered a weed, and its presence extends from the southern United States to some areas of South America; the species *Argemone pleiacantha*, together with other species of the same genus, is known as “chicalote”. Oil physical and chemical properties confirm that chicalote oil is an effective raw material for biofuel production, presenting a fatty acid composition similar to that of soybean oil. A biodiesel production study was carried out using two methods of synthesis, conventional and ultrasound-assisted transesterification, employing the same molar ratio and amount of catalyst in both cases. Reaction time and supplied energy during synthesis were compared in batch mode. The results revealed that ultrasound-assisted transesterification has significant advantages over the conventional one in terms of reaction time and energy savings during chicalote oil synthesis to produce fatty acid methyl esters.

**Keywords:** bioenergy; ultrasound; non-edible oils; chicalote



**Citation:** Sáez-Bastante, J.; Carmona-Cabello, M.; Villarreal-Ornelas, E.; Trejo-Calzada, R.; Pinzi, S.; Dorado, M.P. Feasibility of the Production of *Argemone pleiacantha* Ultrasound-Assisted Biodiesel for Temperate and Tropical Marginal Areas. *Energies* **2023**, *16*, 2588. <https://doi.org/10.3390/en16062588>

Academic Editor: João Fernando Pereira Gomes

Received: 15 February 2023

Revised: 6 March 2023

Accepted: 7 March 2023

Published: 9 March 2023



**Copyright:** © 2023 by the authors. Licensee MDPI, Basel, Switzerland. This article is an open access article distributed under the terms and conditions of the Creative Commons Attribution (CC BY) license (<https://creativecommons.org/licenses/by/4.0/>).

## 1. Introduction

The increasing need to reduce CO<sub>2</sub> emissions to mitigate the effects of global warming, together with the fact that petroleum-derived fuels are an exhaustible energy source, has led to the search for alternative energy sources. The relative simplicity and versatility of the physical (fractionation) or chemical (hydrogenation or transesterification) processes, used separately or combined, allow vegetable oil properties to be modified to make them suitable to be transformed into different kinds of biofuel. Chemically speaking, biodiesel is composed of alkyl esters of fatty acids [1].

Triglycerides (non-polar nature) and short-chain alcohols (polar nature) are chemically antagonistic. For this reason, the reaction mixture needs to be vigorously stirred to make the reagents come into contact with each other as intimately as possible. Subsequently, significant reaction time and temperature are necessary [2]. Moreover, important gaps in biodiesel operating technologies still need to be fixed [3]. In this context, ultrasound constitutes auxiliary energy to enhance transesterification reactions under mild conditions [4,5]. Similar to other energy sources, i.e., microwaves and advanced reactors [6–8], it can be considered among the eco-friendly physical technologies. It is considered a cutting-edge technology based on the improvement of molecule transport phenomena. This intensification process presents a wide range of advantages, i.e., the possibility of using milder processing conditions, the acceleration of reaction rates and the total or partial replacement of the catalyst [3,9].

Transesterification has been carried out in ultrasonic baths, probes and reactors [10,11]. Ultrasonic probes allow the effects of both amplitude and duty cycle on ester yield, besides direct ultrasonication, to be assessed. Amplitude is directly proportional to the power applied to the reaction mixture, while duty cycle refers to the fraction of time in which the sample is ultrasonicated.

Another important issue in biodiesel production is raw material selection. Nowadays, oilseed crops provide more than 70% of world biodiesel production. Therefore, edible crops have been intensely used as raw materials for biodiesel synthesis [12]. However, the production of biodiesel from edible oils is controversial, as some social movements link it with food price rise, soil impoverishment and deforestation of local species [13]. In recent years, other non-edible oleaginous plants, including waste residues, have been explored [14–16]. Preferred species include *Ricinus communis*, *Jatropha curcas*, *Pongamia pinnata* and *Camelina sativa* [17,18].

In this context, *Argemone pleiacantha* is a non-edible species belonging to the *Papaveraceae* family. It mainly grows in warm and dry areas of America, especially in northern Mexico and southwest of the States. In Mexico, it is known as “chicalote” or “cardo santo”.

Usually, *A. pleiacantha* is considered a weed. It flourishes in agricultural areas, besides arid places, road margins and abandoned land. Seeds are employed in infusions due to analgesic, laxative and sedative properties [19]. *A. pleiacantha* may be considered a candidate feedstock for biodiesel production, because it is a non-edible and low-cost raw material (around 80% of final biodiesel cost arises from raw material [12]) that grows in marginal lands and requires little care, showing high oil yield.

In recent years, some species of the genus *Argemone* have been tested for both biodiesel production [20,21] and their use in internal combustion engines, with successful results [22–24]. Sharma et al. [25] and Rao et al. [26] carried out homogeneous and heterogeneous catalyzed transesterification of *A. mexicana* oil, reaching yields over 90% (*w/w*), even exceeding the EN14214 minimum yield threshold in some cases. Fatima et al. tested *A. ochroleuca*, reaching the biodiesel conversion of 91% (*w/w*) after a 120 min reaction, at 65 °C and using a 7:1 methanol-to-oil molar ratio [27]. Agarwal et al. reported a significant reaction time reduction (almost 75%) using microwave-assisted heterogeneously catalyzed transesterification compared with conventional transesterification [28].

In the present work, the suitability of *A. pleiacantha* species for biodiesel production was evaluated. In addition, the conventional transesterification method and the ultrasonicated process, using a probe as an ultrasound (US) device, were compared. The study ranged from oil extraction to biodiesel synthesis and characterization. Response surface methodology modeling and desirability function were used as optimization methods. Finally, biodiesel properties were measured according to European biodiesel standard EN14214.

## 2. Materials and Methods

### 2.1. Materials

#### 2.1.1. Raw Material

Chicalote oil was grown and harvested at San Isidro farm (Chapingo, Mexico). Cultivation and plant processing were carried out by both the Soil, Water and Plant laboratory and the Biotechnology laboratory of Autonomous University of Chapingo.

#### 2.1.2. Reagents for Fatty Acid Composition, Transesterification and Analysis of Both Oil and Biodiesel

Fatty acid determination required 0.1 N sodium methoxide solution, purchased from Sigma-Aldrich Aldrich (Steinheim, Germany), and hexane, supplied by JT Baker (Center Valley, PA, USA). Transesterification reactions required methanol (99% purity) and potassium hydroxide (85% purity; Panreac Química, Barcelona, Spain). The quantification of fatty acid methyl esters (FAME) was carried out using methyl heptadecanoate as internal standard, while mono-, di- and triglyceride (MG, DG and TG, respectively) and glycerol (GLY) contents were analyzed using the following reagents: pyridine, 1,2,4-butanetriol,

1,2,3-tricaproyl glycerol (tricaprine), N-Methyl-N-(trimethylsilyl) and trifluoroacetamide (MSTFA), and all of them were purchased from Sigma-Aldrich. Acid value determination required the use of 2-propanol, toluene and phenolphthalein, and all were acquired from Panreac Química and JT Baker.

#### 2.1.3. Equipment to Characterize Oil and Biodiesel Samples

Water content determination was carried out using a Karl Fischer Coulometer DL32 automatic titrator (Mettler-Toledo, Schawerzenbach, Switzerland). The higher calorific value (HCV) was calculated using an IKA calorimeter bomb (model C200; Staufen, Germany). Carbon residue measurements were conducted using a micro carbon residue tester (model MCRT-160; PAC, Houston, TX, USA). Flash point values were measured using a Seta Flash series 3 plus device acquired from Instrumentación Analítica (Madrid, Spain). The cold filter plugging point (CFPP) was measured using an HCP 842 analyzer purchased from Herzog (Lauda-Königshofen, Germany). Finally, oxidation stability was determined with a Rancimat Metrohm device (Herisau, Switzerland).

#### 2.1.4. Heater–Stirrer

Conventional transesterification was held in a reactor, supported with a heater–stirrer (300–1200 rpm; model Ovan MBG05E (500 W); Espier Group, Barcelona, Spain).

#### 2.1.5. Ultrasonic Probe

Chicalote oil was ultrasonicated using a sonicator (model Q700; 0.5 in (1.27 cm) in diameter) made up of titanium alloy purchased from QSonica LLC (Newtown, CT, USA). The probe allows both continuous and discontinuous ultrasonication, as well as tuning both amplitude and duty cycle, to be performed. It also allows different programs to be performed, making it possible to apply them one after another, with the possibility of introducing a delay between them. To carry out further energy consumption studies, data of applied power and energy consumption were considered.

#### 2.1.6. Equipment for Transesterification Energy Consumption Studies

Power measurements were carried out following the methodology described by Sáez-Bastante et al. [29]. In this sense, two types of analyzers were used. A 435 three-phase power quality analyzer and a 43B analyzer. They were provided by Fluke (Everett, WA, USA).

#### 2.1.7. Chromatographic Analysis

To determine FAME yield and glyceride concentration, methodology and materials were already described in Sáez-Bastante et al. [2]. In this sense, a Perkin-Elmer chromatograph (Clarus 500) coupled to a flame ionization detector (GC-FID) was used. FAME determination required an SGE BPX70 capillary column (30 m in length, 0.32 mm in internal diameter and 0.25  $\mu\text{m}$  thick). Glyceride concentration determination was carried out using an SGE BPX5 capillary column (12 m in length, 0.32 in inner diameter and 0.25  $\mu\text{m}$  film).

### 2.2. Methods

#### 2.2.1. Location, Seeding and Harvesting

The agricultural study was carried out by both the Soil, Water and Plant laboratory and the Biotechnology laboratory of Autonomous University of Chapingo (Mexico). Seed collection was manually performed at San Isidro farm; its geographical coordinates were 25°51'23.5" N and 103°45'56.7" W. The whole plant was extracted and placed on plastic films to finish the drying process, and fruits expelled all seeds; later, seeds were collected and stored in plastic bags. Figure S1 (Supplementary Data) shows a picture of the process.

#### 2.2.2. Grain Milling, Moisture Determination and Oil Extraction

Before the amount of oil was calculated, seed moisture (%) was determined by drying seeds at 105 °C for 4 h. Chicalote seed milling was first conducted by pre-pressing, following

Mexican standard NMX-F-089-S-1978, using a thermo-scientific industrial mill (model 3383-L20), supplied by Thomas Scientific (Swedesboro, NJ, USA). The aim was to expose, as much as possible, triglycerides for further extraction. Once the milling process was finished, oil was obtained with solid–liquid extraction, using a Soxhlet extractor and hexane as solvent. Then, hexane was separated from oil using a rotary evaporator.

### 2.2.3. Fatty Acid Characterization

A small quantity of chicalote oil (0.1 g) was placed in a 12 mL vial; then, 5 mL of hexane was added and stirred for 30 s using a vortex. Later, 0.5 mL of 0.1 N sodium methoxide solution was added. Finally, the solution was centrifuged, and the upper layer was analyzed using a GC-FID according to standard EN14103 [30].

### 2.2.4. Characterization of Oil and Biodiesel Samples

The flash point was measured following the EN ISO 2719 standard; the water content was analyzed according to the EN ISO 12937 specification; carbon residue determination was conducted according to EN ISO 10370; the HCV was calculated according to the ASTM D240 standard; oxidation stability was measured according to the EN14112 regulation; the acid value was obtained following EN ISO 660; the CFPP was analyzed following the EN 116 norm; finally, density and kinematic viscosity were measured following the EN ISO 3675 and EN ISO 3104 standards, respectively. FAME yield was monitored following the EN14103 standard, while glyceride content was measured according to standard EN14105.

### 2.2.5. Acid-Catalyzed Esterification Pretreatment

When the oil acid value shows a high value ( $\geq 3\%$  *w/w*), a two-step reaction is needed [31]. In this case, acid esterification was carried out considering a previous study. The reaction conditions were 10% (*w/w*) of acid catalyst ( $\text{H}_2\text{SO}_4$ ) and 9:1 methanol-to-oil molar ratio, at 65 °C and 60 min of reaction time [32].

### 2.2.6. Ultrasonicated Transesterification

Transesterification was carried out in batch mode. In total, 15 g of chicalote oil was weighed and placed in a wide-mouth flask. Then, a solution of KOH and methanol was added, and ultrasonic transesterification was carried out after selecting the appropriate time. The ultrasonication of the reaction mixtures was carried out discontinuously, introducing a maximum of six stops.

Once the process was completed, samples were centrifuged for five min at 3500 rpm, and biodiesel (upper layer) was separated from glycerol. Each biodiesel sample was washed with distilled water and dried by adding 2.5 g of sodium sulfate anhydrous to remove excess of moisture. Later, samples were centrifuged again, filtered through a 22  $\mu\text{m}$  filter to remove solids in suspension and placed in a vial for further analysis.

### 2.2.7. Conventional Transesterification

Conventional transesterification was carried out in flasks (including water recirculation to avoid methanol losses due to evaporation) under agitation and heating conditions. The transesterification procedure is depicted more in depth in previous works [33]. For chromatographic analysis, samples followed the same treatments as those described for ultrasonicated samples.

### 2.2.8. Energy and Power Measurements

Energy consumption values were calculated at the ultrasonic probe interface. Power measurements were carried out by connecting the heater–stirrer device to a Fluke 435 analyzer. To manage the voltage and frequency of the outlet electric current, a Fluke 43B analyzer was connected to electric current. Working voltage and frequency were 230 V and 50 Hz, respectively.

The energy use index (EUI) is a parameter that allows the reaction energy efficiency to be evaluated and relates the fuel energy released inside an internal combustion engine and the energy supplied in fuel synthesis. The EUI was calculated following the method described by Sáez-Bastante et al. [17,29].

#### 2.2.9. Response Surface Methodology Modeling and Desirability Function as Optimization Method

To optimize the reaction parameters, response surface methodology (RSM) was used. This procedure is an experimental and analytical strategy that allows the optimal process operating conditions to achieve optimal values to be found, thus determining the quality of the desired product [34].

In case of biodiesel production, product quality is linked to FAME yield, and glyceride and glycerol concentrations. The experimental parameters (amplitude, duty cycle and ultrasonication time) were chosen according to previous works in this research field [35]. The selected model, after preliminary tests, was a second-order design called Box–Behnken, with which the response surface can be properly characterized, including the curvature.

The optimization process was carried out using the desirability function method, which involves seeking an optimum graphic point, the center of the small feasible region, which is reached after narrowing original response specifications towards ideal values. It consists in defining a function that estimates the global product desirability at each point and converting a multivariate optimization problem into a univariate optimization problem. To define the global desirability function, each predicted response needs to be transformed into a value of individual desirability that falls in the interval.

### 3. Results

#### 3.1. Chicalote Oilseed Yield, Fatty Acid Composition and Oil Characterization

After oil extraction, the chicalote oil yield was calculated. As may be appreciated in Table 1, the oil yield reached almost 40% ( $w/w$ ). This value is in agreement with those of other common species used in biodiesel production and is slightly lower than those of some oleaginous crops, such as rapeseed, soybean and palm kernel, which present yield values above 40% in weight. However, it is significantly higher than those of other non-edible oils, such as *C. sativa* (30.5%,  $w/w$ ) [36] and *Sinapis alba* oils (25%,  $w/w$ ) [37].

Table 1 also includes the fatty acid composition of chicalote oil. It may be seen that the chicalote oil density and viscosity values are comparable to those of oils depicting similar unsaturation degrees, i.e., rapeseed and soybean oils [2]. Moreover, as previously mentioned in Section 2.2.5, it may be seen that the oil acid value is high, above 3% ( $w/w$ ), thus indicating that acid pretreatment before transesterification is needed.

In addition, Figure 1 shows a comparison between chicalote oil fatty acid composition (highlighted in red) and that of other oils. In the figure, the positive values correspond to saturated fatty acids, while the negative values indicate unsaturated ones. Considering the three leading oils in biodiesel production (rapeseed, soybean and palm oil), chicalote oil shows higher similarity with soybean, because it presents a similar content of both linoleic and palmitic acids. On the other hand, considering non-edible oils, chicalote oil presents a significant advantage over *Camelina sativa*, due to the high content of linolenic acid of the latter. As high linoleic acid content may lead to oil oxidation, its concentration is limited to 12% ( $w/w$ ) according to European standard EN14214. Figure 1 shows information about the fatty acid composition of *A. pleiakantha* greene, another species with fatty acid composition almost identical to that of *A. pleiakantha*, although showing a higher content of linoleic acid.

**Table 1.** Chicalote oilseed characterization, fatty acid composition, and some physical and chemical properties.

Oilseed Characterization		
Oilseed yield (% w/w)	39.81	
Moisture (% w/w)	5.57	
Fatty Acid Composition		
Fatty Acid	Content (% w/w)	
Myristic acid (C14:0)	0.10	
Palmitic acid (C16:0)	13.22	
Palmitoleic acid (C16:1)	0.77	
Stearic acid (C18:0)	4.22	
Oleic acid (C18:1)	22.79	
Linoleic acid (C18:2)	58.17	
Linolenic acid (C18:3)	0.73	
Hydrocarbon Chain Properties		
LC <sup>1</sup>	17.71	
TUD <sup>2</sup>	143.55	
PUD <sup>3</sup>	58.90	
MUD <sup>4</sup>	23.56	
Physical and Chemical Properties		
Water content (ppm)	510	
Acid value (mg KOH/g)	Before AT <sup>5</sup> 14.58	After AT 0.28
Density (kg/m <sup>3</sup> )	928	
Kinematic viscosity (mm <sup>2</sup> /s)	27.15	

<sup>1</sup> LC: length of chain, with  $LC = \sum(nC_n)/100$ , where n is the number of carbon atoms of each fatty acid and Cn is the weight percentage of each methyl ester in the given fatty acid. <sup>2</sup> TUD: total unsaturation degree, with  $TUD = (1\%MU + 2\%DU + 3\%TU)$ , where %MU is the weight percentage of monounsaturated methyl esters, %DU is the weight percentage of diunsaturated methyl esters and %TU is the weight percentage of triunsaturated methyl esters. <sup>3</sup> PUD: polyunsaturation degree. <sup>4</sup> MUD: monounsaturation degree. <sup>5</sup> AT: acid transesterification.

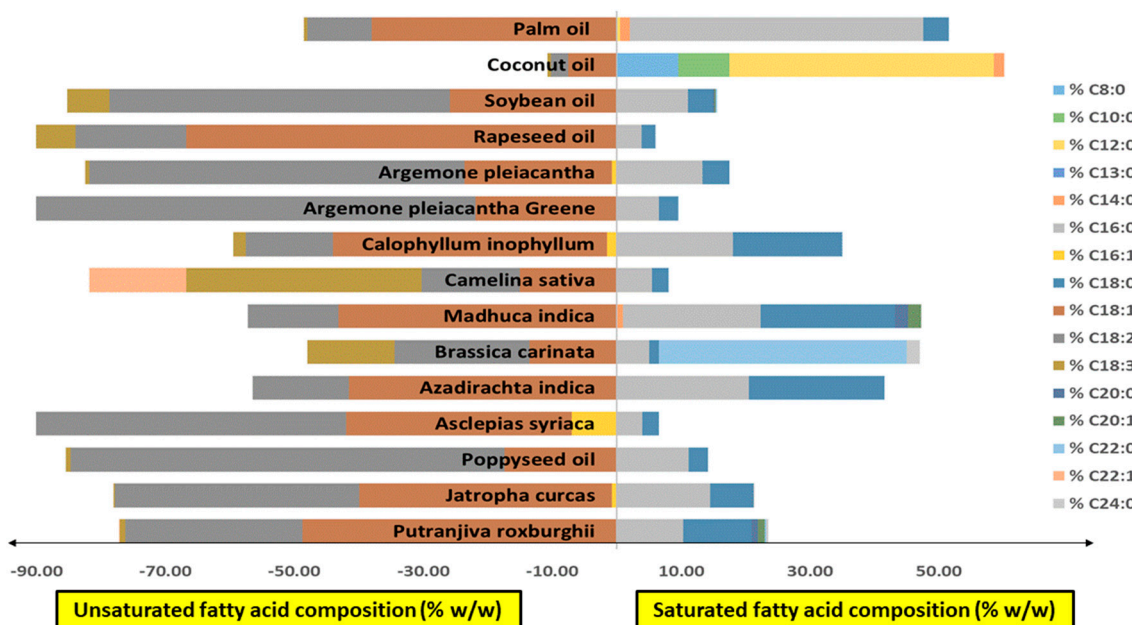


**Figure 1.** Comparison between chicalote oil fatty acid composition, and that of other non-edible oils and the top three oils in biodiesel production. The positive values correspond to saturated fatty acids, and the negative ones to unsaturated fatty acids.

### 3.2. Previous Acid Esterification

Raw material free fatty acid concentration is a key parameter to take into consideration when a basic transesterification reaction is carried out, especially in the presence of alkaline metals, i.e., sodium or potassium. In fact, they can react with non-esterified acidic groups, leading to subsequent soap formation. The chicalote oil acid value is 14.58 mg KOH/g (Table 1), which corresponds with an acid value of 7.36% (*w/w*). This value is much higher than the maximum recommended value reported by Dorado et al. [31], which should be less than 3% (*w/w*) to avoid soap formation.

Therefore, to reduce as much as possible the concentration of free fatty acids, a previous acid esterification step was needed. Subsequently, this resulted in higher FAME conversion. Once this process was finished, the acid value was reduced from 14.58 to 0.28 mg KOH/g (Table 1), which constitutes an adequate value to perform basic transesterification.

### 3.3. Basic Transesterification

#### 3.3.1. Ultrasonicated Transesterification

- Response surface modeling

To gain knowledge about the influence of three experimental US factors (amplitude, duty cycle and ultrasonication time) on five reaction response variables (FAME, MGs, DGs, TGs and GLY), a Box–Behnken design was elaborated. The design was run in a single block (15 runs, including three center points and five degrees of freedom), and the order of the experiments was fully randomized to avoid the effects of lurking variables. In addition, the methanol-to-oil molar ratio and the catalyst concentration were set to 6:1 and 1.5% (*w/w*), respectively, considering previous research works [2,25]. As may be observed in Table S1 (supplementary data), higher FAME concentrations usually corresponded to high and medium reaction time; some yields exceeded 96.5% (*w/w*), which is the minimum threshold established by European biodiesel standard EN14214. This trend was also observed in all response variables.

Following the above methodology and using the software described in Section 2.2.9, analysis of the variance (ANOVA) was carried out; each response variable was individually considered. Table S2 (Supplementary Data) shows the effects of the experimental parameters on the response variables, considering an alpha value of 0.05. Table S2 also reports the error values, *p*-values and coefficients of the determination of the estimated effects. The ANOVA table partitioned FAME variability into separate parts for each of the effects of the experimental parameters on the response variables. Then, the statistical significance of each effect was tested by comparing mean square against error estimation. In this case, eight effects had *p*-values below 0.05, indicating that they were significantly different from zero at the 95.0% confidence level.

Considering FAME conversion, all experimental parameters presented a positive and significant effect, meaning that by increasing these factors, a significant increase in FAME conversion may be expected. In the case of triglycerides, all experimental parameters consistently presented a negative response, although not significant. The remaining glycerides had negative and positive tendencies, with negative responses predominating, as expected. Only in the case of monoglycerides, for duty cycle and amplitude, a significant negative response was achieved, meaning that an increase in probe duty and amplitude may cause a significant (at the 95% confidence level) reduction in MGs. A summary of signs and significance of the experimental parameters is shown in Table S2.

- Desirability approach
- The desirability function converts an estimated response into a scale-free value. Its value varies between 0 and 1 and increases as the corresponding response value becomes more desirable. The overall desirability, *D* (0 and 1) is defined by combining individual desirability values. The optimal setting is determined by maximizing *D*. The calculation for this function is expressed in Equation (1).

$$d_i(\hat{y}_i(x)) = \begin{cases} 0 & \text{if } \hat{y}_i(x) \leq Y_i^{\min} \text{ or } \hat{y}_i(x) > Y_i^{\max}, \\ \left( \frac{\hat{y}_i(x) - Y_i^{\min}}{T_i^{\min} - Y_i^{\min}} \right)^{s_i} & \text{if } Y_i^{\min} < \hat{y}_i(x) \leq T_i^{\min}, \\ \left( \frac{Y_i^{\max} - \hat{y}_i(x)}{Y_i^{\max} - T_i^{\max}} \right)^{t_i} & \text{if } T_i^{\max} < \hat{y}_i(x) \leq Y_i^{\max}, \\ 1 & \text{if } T_i^{\min} < \hat{y}_i(x) \leq T_i^{\max}, \end{cases} \quad (1)$$

where  $d_i$  is the desirability function of  $y$ ,  $Y$  corresponds to the lower and upper bounds of the response,  $T$  relates to the lower and upper targets of the response, and  $s_i$  and  $t_i$  are parameters that determine the shapes of the desirability function.

After evaluating the response variable results, the optimum operation value that can produce biodiesel under the most favorable conditions was sought out. The evaluated variables (amplitude, duty cycle and ultrasonication time) showed different operating ranges, so a joint response that encompassed all variables in the same range was targeted. The selected optimization method was the desirability function approach. Individual desirability and overall desirability evaluate how a combination of variables satisfies previously defined goals for response variables. Individual desirability evaluates the way in which a configuration optimizes an individual response. Overall desirability evaluates the way in which a configuration optimizes a set of responses, providing a value in the range from zero to one (one represents the ideal situation, while zero indicates that one or more responses are outside the acceptable limits). In the case of biodiesel production, the final product quality demands the maximization of some responses and the minimization of others. This procedure helps to determine the combination of experimental parameters that simultaneously optimize several responses while maximizing the desirability function. In Table 2, the goals for each response variable (maximized or minimized) and each run are provided; maximum desirability was achieved at run 11.

**Table 2.** Response variable limits and desirability values for each experiment considering EN14214. MGs, monoglycerides; DGs, diglycerides; TGs, triglycerides; FAME, fatty acid methyl esters.

Response Variable	Low	High	Goal
MGs (% $w/w$ )	0.055	0.70	Minimizing
DGs (% $w/w$ )	0.12	0.20	Minimizing
TGs (% $w/w$ )	0.033	0.20	Minimizing
FAME (% $w/w$ )	96.50	98.45	Maximizing

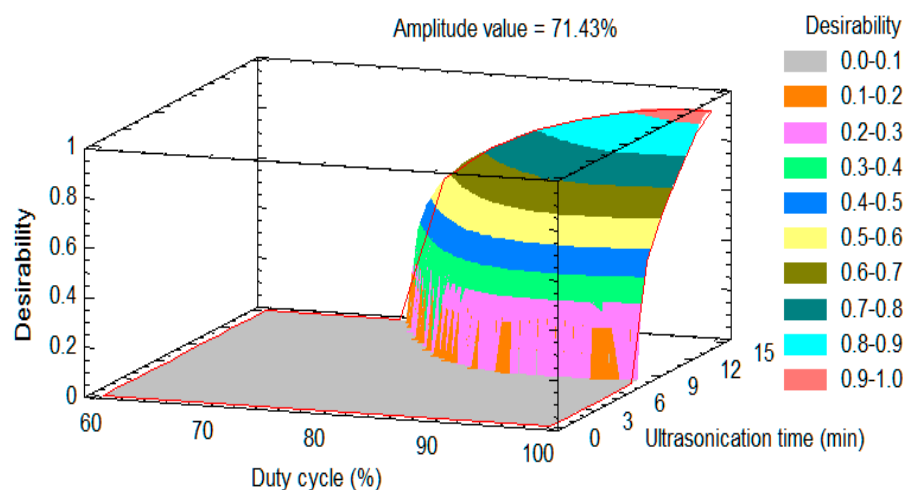
To carry out the desirability study, the minimum threshold of FAME conversion was set to 96.50% ( $w/w$ ), in agreement with European biodiesel standard EN14214. The same criterion was used to establish maximum glyceride concentration limits.

Under these conditions, it was possible to establish a range of operation where the synthesized biodiesel met quality requirements. Table 3 shows the combination of factor levels that maximized the desirability function over the indicated limits and the combination of factors that provided the optimum. As can be seen, the optimal values correspond to almost the upper limits of both duty cycle and amplitude, which are coincident with the upper limit of ultrasonication time. This combination of parameters can lead to optimal biodiesel production. Table 3 also provides the concentration (%  $w/w$ ) of each response variable under optimal operating conditions. In this case, it is very important to remark that all response variables satisfy thresholds established by European biodiesel standard EN14214.

**Table 3.** Optimum values for experimental parameters and response variables at maximum desirability value. MGs, monoglycerides; DGs, diglycerides; TGs, triglycerides; FAMES, fatty acid methyl ester.

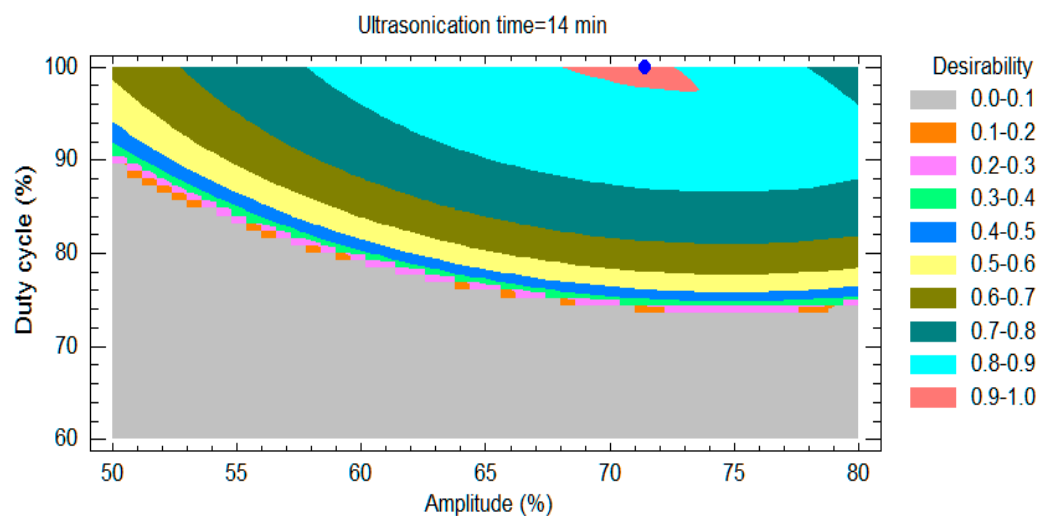
Experimental Parameter	Low	High	Optimum
Amplitude (%)	50.00	80.00	71.43
Duty cycle (%)	60	100	100
Ultrasonication time (min)	2	14	14
Response Variable	Predicted Optimum Value	Experimental Optimum Value	EN 14214 Limit
MGs (% w/w)	0.190	0.10	≤0.70
DGs (% w/w)	0.055	0.12	≤0.20
TGs (% w/w)	0.039	0.040	≤0.20
FAME (% w/w)	98.30	98.45	≥96.50
Desirability optimum value		0.91	

Figure 2 shows the 3D response surface for the optimal amplitude value of 71.43%, providing desirability values with respect to duty cycle and ultrasonication time. As can be appreciated, the desirability maximum value is achieved with maximum ultrasonication time (14 min) and duty cycle (100%) values, as expected.



**Figure 2.** Response surface for optimal amplitude value.

Moreover, Figure 3 includes the corresponding 2D contour surface response, considering the optimal ultrasonication time (14 min). In these figures, EN14214 is used to provide FAME yield and glyceride concentration thresholds in the desirability study, as shown in Table 2. For this reason, only the region where the European standard is fulfilled is represented. The gray area (with a desirability value of zero) does not simultaneously satisfy these requirements, so it should be neglected in biodiesel production. The colored regions (with non-zero desirability values) represent areas where biodiesel that meets EN14214 may be produced. In this way, if the duty cycle values are equal to or above 90%, suitable biodiesel (meeting European standard EN14214) may be produced using amplitudes in the range of 50–80%. It is important to remark that this makes it possible to work at low amplitudes and duty cycles, which are linked to significant energy saving in biodiesel production, since the power applied to the samples and, subsequently, energy consumption are directly related to these variables.



**Figure 3.** Contour surfaces for optimal ultrasonic time value. Dark blue point: desirability optimal value.

Finally, the light-red region corresponds to optimum desirability function values (range 0.9–1) that achieve the desirability optimal value (0.91) highlighted with a single dark blue point. This point represents the best conditions to produce biodiesel. Consistently, it corresponds with 100% duty cycle value and 71.43% amplitude value, as predicted in the desirability study and shown in Table 3.

### 3.3.2. Conventional Transesterification

To establish a comparison between conventional and ultrasonicated transesterification, in terms of both FAME yield and energy consumption, a kinetic study was carried out. The same catalyst concentrations and methanol-to-oil molar ratios were used in both reactions. The temperature and agitation conditions were 55 °C (below methanol boiling point) and 900 rpm, respectively.

Reactions were carried out in flasks with refluxing water to prevent the temperature from rising above 55 °C, and to stop the reactions completely once the final reaction time was reached, the flask with the reaction mixture was immersed in ice-cold water with ethylene glycol. Aliquots were collected after 5, 15, 30, 40, 50 and 60 min of reaction. Figure 4 shows FAME yield vs. reaction time, and the maximum conversion was reached after 60 min. Reaction time over this value did not increase conversion above 97%. It is remarkable that a significant conversion increase occurred from 40 to 50 min. Usually, the highest conversion takes place in the first reaction minutes. Then, it continues increasing to a lesser extent until reaching a final plateau, without significant conversion around 45–60 min of reaction, depending on oil type and reaction conditions. In this case, the kinetic study depicted a similar behavior. However, from 5 to 40 min of reaction, FAME conversion did not fulfill European biodiesel standard EN14124.

On the other hand, considering both FAME conversion and the desirability study for ultrasound-assisted transesterification, it may be seen that ultrasonicated transesterification allowed higher FAME conversion to be achieved in shorter reaction time than conventional (heated and stirred) alkali-catalyzed transesterification.

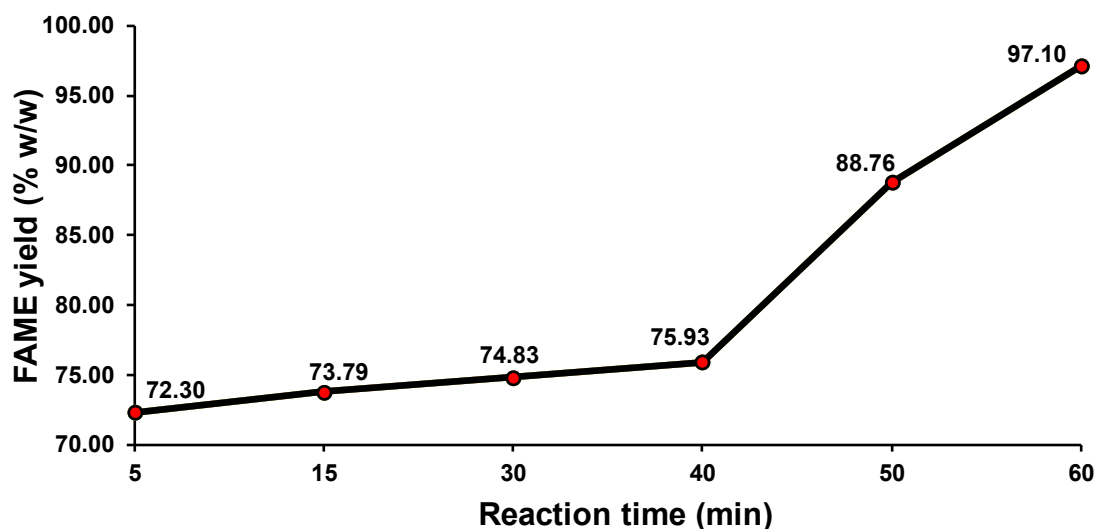


**Figure 4.** Kinetic studies of chicalote oil transesterification using conventional reaction (heating–stirring method).

### 3.3.3. Energy Consumption Study and Regulated Quality Parameters

New tendencies in biodiesel production demand energy and time savings with respect to the conventional method. For this reason, to introduce alternative technologies in biodiesel production, previous energy comparative studies are recommended.

In previous works on biodiesel synthesis, data related to the energy consumed in the process, as well as the comparison with conventional transesterification, have been reported [17,29,35]. Considering the same energy consumed in the previous acid esterification step, in both US-assisted and conventional transesterification reactions, a comparison between the EUIs calculated for the optimal biodiesel values showed a higher value (1.20) for ultrasonicated transesterification than for the conventional one (0.57). The results show that the ultrasonicated reaction was more than two times more energetically efficient than the conventional one (Table S3, Supplementary Data).

Moreover, some of the most representative physical and chemical properties that characterize biodiesel quality were determined following European regulations. In Table 4, the values of these properties measured considering optimal values for each type of transesterification are shown. As can be seen, most evaluated parameters meet regulations (including FAME, and mono-, di- and triglycerides; Table 3), except for the oxidation stability value and glycerol content, which are below and above the thresholds established by European biodiesel standard EN14214, respectively. The oxidation of biodiesel may lead to hydroperoxide formation, which may be responsible for sediments and gums that can plug fuel filters and produce deposits in injectors. Moreover, oxidized products increase viscosity, causing poor fuel atomization [38]. Polycyclic aromatic hydrocarbon (PAH), formaldehyde and acetaldehyde increases in exhaust emissions are observed in engines fueled with oxidized biodiesel [39]. For this reason, improving biodiesel stability is key; the most cost-effective way is the use of a small amount of antioxidant. The effectiveness of antioxidant additives depends on biodiesel chemical composition, and the *A. pleiakantha* oil fatty acid profile is similar to that of soybean oil (Figure 1). So, the same antioxidants may be used. In this sense, pyrogallol or tert-Butylhydroquinone have been presented as the most effective antioxidants for soybean oil biodiesel [38,40]. In addition, total glycerol content is high. This may lead to inadequate combustion and subsequent deposits in the injectors. The higher calorific value of chicalote oil biodiesel is comparable with that from other kinds of biodiesel, i.e., soybean, palm or rapeseed oil biodiesel. The cetane number was predicted using mathematical models, providing a value above the minimum threshold [41].

**Table 4.** Quality properties for ultrasonicated and conventional reaction optimal values.

Property	Biodiesel Standard EN14214	Ultrasonicated Reaction	Conventional Reaction
Total glycerol content (% <i>w/w</i> )	EN14105 Max: 0.25	0.38	0.42
Water content (ppm)	EN ISO 12937 Max: 500	390	410
Carbon residue remnant (% <i>w/w</i> )	EN ISO 10370 Max: 0.3	0.12	0.18
Flash point (°C)	EN ISO 2719 Min: 101	140	140
Higher calorific value (J/g)	ASTM D240	38,968	38,395
Kinematic viscosity at 40 °C (mm <sup>2</sup> /s)	EN ISO 3401 Min: 3.5; max: 5	3.90	4.10
Density at 15 °C (kg/m <sup>3</sup> )	EN ISO 3675 Min: 860; max: 900	870	880
Cold filter plugging point (°C)	EN116	−3	−3
Oxidation stability at 110 °C (h)	EN14112 Min: 8 h	1.5	1.5
Cetane number *	Min: 51	55.30	55.30

\* Calculated from Pinzi et al.'s [41] method; cetane number depends on fatty acid composition.

No significant differences between properties for ultrasonicated and conventional reaction optimal values were found, although the optimal biodiesel value achieved using US-assisted transesterification presented slightly better behavior than that achieved with the conventional reaction.

EN 590 includes physical properties that automotive diesel fuel must meet if it is sold in the EU, Croatia, Iceland, Norway and Switzerland. Depending on the value of some properties, diesel fuel is classified in different groups, according to climate conditions. The cold filter plugging point (CFPP) value of biodiesel resulting from both reactions was −3 °C. Although EN14214 does not include any limit to this property, considering the EN 590 standard, chicalote oil biodiesel belongs to temperate climatic zones (class B).

In summary, this biodiesel satisfies the evaluated standard, except for the glycerol content and oxidation stability. However, as, in the EU, biodiesel is used in mixtures with diesel fuel, in which the maximum percentage of biodiesel is 10% *v/v*, it can be safely used.

#### 4. Conclusions

Considering the variability in regions where this plant grows, it can be concluded that *A. pleiacantha* oil is suitable as raw material in the biodiesel industry, though requiring a previous acid-catalyzed esterification step. The fatty acid composition is similar to that of soybean oil. Compared with conventional transesterification, the ultrasound (US)-assisted reaction provides higher biodiesel yields in shorter reaction time, besides energy savings. The higher the duty and amplitude of the ultrasonic probe are, the better the quality of FAME from *A. pleiacantha* is, when using US-assisted transesterification. Moreover, with the exception of oxidation stability and total glycerol content, FAME from *A. pleiacantha* show chemical and physical properties that fulfill the European biodiesel quality standard and could be marketed in the EU by blending them with diesel fuel.

**Supplementary Materials:** The following supporting information can be downloaded at: <https://www.mdpi.com/article/10.3390/en16062588/s1>, Figure S1. Drying process; Table S1. Design of experiments and results for response variables after experimentation. FAME: fatty acid methyl esters; MG: monoglycerides; DG: diglycerides; TG: triglycerides; Table S2. Estimated effects of experimental parameters on response variables and ANOVA analysis; Table S3. Energy consumption

and Energy Use Index (EUI) for ultrasound-assisted and conventional transesterification reactions at optimal values.

**Author Contributions:** Conceptualization, J.S.-B., S.P., R.T.-C. and M.P.D.; methodology, J.S.-B., S.P. and M.P.D.; formal analysis, J.S.-B. and M.C.-C.; investigation, E.V.-O. and M.C.-C.; writing—original draft preparation, J.S.-B.; writing—review and editing, S.P. and M.P.D. All authors have read and agreed to the published version of the manuscript.

**Funding:** This research was funded by the Spanish Ministry of Economy and Competitiveness (grant No. PID2019-105936RB-C21) and the Spanish Ministry of Science and Innovation (TED2021-130596B-C22).

**Data Availability Statement:** Data is fully provided in this manuscript.

**Acknowledgments:** The authors acknowledge the Spanish Ministry of Economy and Competitiveness (grant No. PID2019-105936RB-C21) and the Spanish Ministry of Science and Innovation (TED2021-130596B-C22).

**Conflicts of Interest:** The authors declare no conflict of interest.

## References

1. Costarrosa, L.; Leiva-Candia, D.E.; Cubero-Atienza, A.J.; Ruiz, J.J.; Dorado, M.P. Optimization of the transesterification of waste cooking oil with Mg-Al hydrotalcite using response surface methodology. *Energies* **2018**, *11*, 302. [[CrossRef](#)]
2. Sáez-Bastante, J.; Pinzi, S.; Arzamendi, G.; Luque de Castro, M.D.; Priego-Capote, F.; Dorado, M.P. Influence of vegetable oil fatty acid composition on ultrasound-assisted synthesis of biodiesel. *Fuel* **2014**, *125*, 183–191. [[CrossRef](#)]
3. Haghighi, S.F.M.; Parvasi, P.; Jokar, S.M.; Basile, A. Investigating the effects of ultrasonic frequency and membrane technology on biodiesel production from chicken waste. *Energies* **2021**, *14*, 2133. [[CrossRef](#)]
4. Ho, W.W.S.; Ng, H.K.; Gan, S. Advances in ultrasound-assisted transesterification for biodiesel production. *Appl. Therm. Eng.* **2016**, *100*, 553–563. [[CrossRef](#)]
5. Mofijur, M.; Kusumo, F.; Fattah, I.M.R.; Mahmudul, H.M.; Rasul, M.G.; Shamsuddin, A.H.; Mahlia, T.M.I. Resource recovery from waste coffee grounds using ultrasonic-assisted technology for bioenergy production. *Energies* **2020**, *13*, 1770. [[CrossRef](#)]
6. Liu, L.; Hong, Y.; Ye, X.; Wei, L.; Liao, J.; Huang, X.; Liu, C. Biodiesel production from microbial granules in sequencing batch reactor. *Bioresour. Technol.* **2018**, *249*, 908–915. [[CrossRef](#)]
7. Sharma, A.K.; Sahoo, P.K.; Singhal, S.; Joshi, G. Exploration of upstream and downstream process for microwave assisted sustainable biodiesel production from microalgae *Chlorella vulgaris*. *Bioresour. Technol.* **2016**, *216*, 793–800. [[CrossRef](#)]
8. Chellappan, S.; Aparna, K.; Chingakhm, C.; Sajith, V.; Nair, V. Microwave assisted biodiesel production using a novel Brønsted acid catalyst based on nanomagnetic biocomposite. *Fuel* **2019**, *246*, 268–276. [[CrossRef](#)]
9. Tagliapietra, S.; Calcio Gaudino, E.; Cravotto, G. 33-The use of power ultrasound for organic synthesis in green chemistry. In *Power Ultrasonics*; Gallego-Juárez, J.A., Graff, K.F., Eds.; Woodhead Publishing: Oxford, UK, 2015; pp. 997–1022.
10. Asgharzadehahmadi, S.; Raman, A.A.A.; Parthasarathy, R.; Sajjadi, B. Sonochemical reactors: Review on features, advantages and limitations. *Renew. Sustain. Energy Rev.* **2016**, *63*, 302–314. [[CrossRef](#)]
11. Gallego-Juárez, J.A.; Rodríguez, G.; Acosta, V.; Riera, E. Power ultrasonic transducers with extensive radiators for industrial processing. *Ultrason. Sonochemistry* **2010**, *17*, 953–964. [[CrossRef](#)]
12. Pinzi, S.; Leiva-Candia, D.E.; García, I.L.; Redel-Macías, M.D.; Dorado, M.P. Latest trends in feedstocks for biodiesel production. *Biofuels Bioprod. Biorefining-Biofpr.* **2014**, *8*, 126–143. [[CrossRef](#)]
13. Fadhil, A.B.; Al-Tikrity, E.T.B.; Albadree, M.A. Biodiesel production from mixed non-edible oils, castor seed oil and waste fish oil. *Fuel* **2017**, *210*, 721–728. [[CrossRef](#)]
14. Jung, J.-M.; Lee, S.-R.; Lee, J.; Lee, T.; Tsang, D.C.W.; Kwon, E.E. Biodiesel synthesis using chicken manure biochar and waste cooking oil. *Bioresour. Technol.* **2017**, *244*, 810–815. [[CrossRef](#)]
15. Patiño, Y.; Mantecón, L.G.; Polo, S.; Faba, L.; Díaz, E.; Ordóñez, S. Effect of sludge features and extraction-esterification technology on the synthesis of biodiesel from secondary wastewater treatment sludges. *Bioresour. Technol.* **2018**, *247*, 209–216. [[CrossRef](#)] [[PubMed](#)]
16. Kamil, M.; Ramadan, K.; Olabi, A.G.; Ghenai, C.; Inayat, A.; Rajab, M.H. Desert palm date seeds as a biodiesel feedstock: Extraction, characterization, and engine testing. *Energies* **2019**, *12*, 3147. [[CrossRef](#)]
17. Saez-Bastante, J.; Pinzi, S.; Jimenez-Romero, F.J.; Luque de Castro, M.D.; Priego-Capote, F.; Dorado, M.P. Synthesis of biodiesel from castor oil: Silent versus sonicated methylation and energy studies. *Energy Convers. Manag.* **2015**, *96*, 561–567. [[CrossRef](#)]
18. Patel, C.; Chandra, K.; Hwang, J.; Agarwal, R.A.; Gupta, N.; Bae, C.; Agarwal, A.K. Comparative compression ignition engine performance, combustion, and emission characteristics, and trace metals in particulates from waste cooking oil, Jatropha and Karanja oil derived biodiesels. *Fuel* **2019**, *236*, 1366–1376. [[CrossRef](#)]
19. Xool-Tamayo, J.F.; Graniel-Sabido, M.; Miron-Lopez, G.; Mena-Rejon, G.J.; Monforte-Gonzalez, M.; Flota, F.V. HPLC-DAD Determination of berberine, chelerythrine and sanguinarine in the Mexican prickly poppy (*Argemone mexicana* L. papaveraceae), a medicinal plant. *Quim. Nova* **2017**, *40*, 1238–1243.

20. Singh, D.; Singh, S.P. Low cost production of ester from non edible oil of *Argemone mexicana*. *Biomass Bioenergy* **2010**, *34*, 545–549. [[CrossRef](#)]
21. Pramanik, P.; Das, P.; Kim, P.J. Preparation of biofuel from argemone seed oil by an alternative cost-effective technique. *Fuel* **2012**, *91*, 81–86. [[CrossRef](#)]
22. Singh, M.; Sandhu, S.S. Performance and emission characteristics of an indirect injection (IDI) multi-cylinder compression ignition (CI) engine using diesel/*Argemone mexicana* biodiesel blends. *RSC Adv.* **2015**, *5*, 91069–91081. [[CrossRef](#)]
23. Parida, M.K.; Rout, A.K. Investigation of performance and emission analysis of *Argemone mexicana* biodiesel blends as a fuel in a DIC engine at part load conditions. *Energy Sources Part A-Recovery Util. Environ. Eff.* **2017**, *39*, 623–629. [[CrossRef](#)]
24. Parida, M.K.; Rout, A.K. Combustion analysis of *Argemone mexicana* biodiesel blends. *Energy Sources Part A-Recovery Util. Environ. Eff.* **2017**, *39*, 698–705. [[CrossRef](#)]
25. Sharma, M.; Khan, A.A.; Dohhen, K.C.; Christopher, J.; Puri, S.K.; Tuli, D.K. A heterogeneous catalyst for transesterification of *Argemone mexicana* oil. *J. Am. Oil Chem. Soc.* **2012**, *89*, 1545–1555. [[CrossRef](#)]
26. Rao, R.Y.; Zubaidha, P.K.; Kondhare, D.D.; Reddy, N.J.; Deshmukh, S.S. Biodiesel production from *Argemone mexicana* seed oil using crystalline manganese carbonate. *Pol. J. Chem. Technol.* **2012**, *14*, 65–70. [[CrossRef](#)]
27. Fatima, A.; Zafar, M.; Ahmad, M.; Sultana, S.; Ali, M.I. Parametric characterization and statistical optimization of *Argemone ochroleuca* (Mexican Poppy) methyl esters as a renewable source of energy. *Energy Sources Part A-Recovery Util. Environ. Eff.* **2017**, *39*, 1963–1969. [[CrossRef](#)]
28. Agarwal, S.; Chhibber, V.K.; Bhatnagar, A.K.; Srivastav, B.; Kumar, A.; Singhal, S.; Sharma, A.K. Physico-chemical and tribological studies of *Argemone* biodiesel synthesized using microwave technique. *Curr. Sci.* **2017**, *113*, 938–941. [[CrossRef](#)]
29. Sáez-Bastante, J.; Ortega-Román, C.; Pinzi, S.; Lara-Raya, F.R.; Leiva-Candia, D.E.; Dorado, M.P. Ultrasound-assisted biodiesel production from *Camelina sativa* oil. *Bioresour. Technol.* **2015**, *185*, 116–124. [[CrossRef](#)]
30. Sánchez-Avila, N.; Mata-Granados, J.M.; Ruiz-Jiménez, J.; Luque de Castro, M.D. Fast, sensitive and highly discriminant gas chromatography-mass spectrometry method for profiling analysis of fatty acids in serum. *J. Chromatogr. A* **2009**, *1216*, 6864–6872. [[CrossRef](#)]
31. Dorado, M.P.; Ballesteros, E.; de Almeida, J.A.; Schellert, C.; Lohrlein, H.P.; Krause, R. An alkali-catalyzed transesterification process for high free fatty acid waste oils. *Trans. ASAE* **2002**, *45*, 525–529. [[CrossRef](#)]
32. Saha, R.; Goud, V.V. Ultrasound assisted transesterification of high free fatty acids karanja oil using heterogeneous base catalysts. *Biomass Convers. Biorefinery* **2015**, *5*, 195–207. [[CrossRef](#)]
33. Carmona-Cabello, M.; Leiva-Candia, D.; Castro-Cantarero, J.L.; Pinzi, S.; Dorado, M.P. Valorization of food waste from restaurants by transesterification of the lipid fraction. *Fuel* **2018**, *215*, 492–498. [[CrossRef](#)]
34. Pinzi, S.; López-Giménez, F.J.; Ruiz, J.J.; Dorado, M.P. Response surface modeling to predict biodiesel yield in a multi-feedstock biodiesel production plant. *Bioresour. Technol.* **2010**, *101*, 9587–9593. [[CrossRef](#)]
35. Sáez-Bastante, J.; Pinzi, S.; Reyero, I.; Priego-Capote, F.; de Castro, M.D.L.; Dorado, M.P. Biodiesel synthesis from saturated and unsaturated oils assisted by the combination of ultrasound, agitation and heating. *Fuel* **2014**, *131*, 6–16. [[CrossRef](#)]
36. Moser, B.R.; Vaughn, S.F. Evaluation of alkyl esters from *Camelina sativa* oil as biodiesel and as blend components in ultra low-sulfur diesel fuel. *Bioresour. Technol.* **2010**, *101*, 646–653. [[CrossRef](#)] [[PubMed](#)]
37. Sáez-Bastante, J.; Fernández-García, P.; Saavedra, M.; López-Bellido, L.; Dorado, M.P.; Pinzi, S. Evaluation of *Sinapis alba* as feedstock for biodiesel production in Mediterranean climate. *Fuel* **2016**, *184*, 656–664. [[CrossRef](#)]
38. Varatharajan, K.; Pushparani, D.S. Screening of antioxidant additives for biodiesel fuels. *Renew. Sustain. Energy Rev.* **2018**, *82*, 2017–2028. [[CrossRef](#)]
39. Karavalakis, G.; Bakeas, E.; Stournas, S. Influence of oxidized biodiesel blends on regulated and unregulated emissions from a diesel passenger car. *Environ. Sci. Technol.* **2010**, *44*, 5306–5312. [[CrossRef](#)] [[PubMed](#)]
40. Nogales-Delgado, S.; Maria Encinar, J.; Felix Gonzalez, J. Safflower biodiesel: Improvement of its oxidative stability by using BHA and TBHQ. *Energies* **2019**, *12*, 1940. [[CrossRef](#)]
41. Pinzi, S.; Mata-Granados, J.M.; Lopez-Gimenez, F.J.; de Castro, M.D.L.; Dorado, M.P. Influence of vegetable oils fatty-acid composition on biodiesel optimization. *Bioresour. Technol.* **2011**, *102*, 1059–1065. [[CrossRef](#)]

**Disclaimer/Publisher’s Note:** The statements, opinions and data contained in all publications are solely those of the individual author(s) and contributor(s) and not of MDPI and/or the editor(s). MDPI and/or the editor(s) disclaim responsibility for any injury to people or property resulting from any ideas, methods, instructions or products referred to in the content.